

# A PH-DIFFERENTIAL PHOTOELECTROCHEMICAL SYSTEM FOR BIAS-FREE CARBON DIOXIDE REDUCTION: A MODELING STUDY

Hao Zhang<sup>1</sup>, Huizhi Wang<sup>2</sup>, Jin Xuan<sup>1\*</sup>

<sup>1</sup> Department of Chemical Engineering, Loughborough University, Loughborough, UK

<sup>2</sup> Department of Mechanical Engineering, Imperial College London, London, UK

\* Corresponding Author, j.xuan@lboro.ac.uk

## ABSTRACT

In direct photoelectrochemical reduction of CO<sub>2</sub>, p-type semiconductors are usually used as photocathode to supply light-induced electrons to reduce CO<sub>2</sub>. However, since the band position at the surface of semiconductor is fixed, the overpotential of CO<sub>2</sub> reduction reaction at the interface is unchangeable. Therefore, it is impossible to boost the interfacial reaction through increasing interfacial overpotential. A photoelectrochemical cell (PEC) that consists of an n-type photoanode and a metal cathode offers the opportunity to manipulate the cathode overpotential. Furthermore, by applying different pH values for the anolyte and catholyte, the PEC can be self-contained and no bias voltage is needed.

**Keywords:** photoelectrochemical, photoanode, carbon dioxide reduction

## NONMENCLATURE

### Abbreviations

PEC Photoelectrochemical

### Symbols

$j_{ph}$  Photocurrent  
 $\Phi$  Surface recombination factor  
 $e$  Elementary charge  
 $I$  Photon flux of incident light  
 $\alpha$  Light absorption coefficient  
 $\delta_{sc}$  The thickness of space charge layer  
 $L$  Diffusion length of charge carrier  
 $\epsilon$  Dielectric constant of semiconductor

$\epsilon_0$	Permittivity of vacuum
$\Delta\varphi_{sc}$	The potential difference across the space charge layer
$N_d$	Donor density of semiconductor
$V_{fb}$	Flat band potential
$V$	Potential of photoanode
$R_t, R_r$	Charge transfer resistance and recombination resistance at the surface of semiconductor
$A, B$	Constant factor
$j_{0,c}$	Exchange current density at cathode
$\beta_c$	Transfer coefficient of cathodic reaction
$F$	Faradaic constant
$\eta$	Overpotential
$R$	Universal constant
$T$	Temperature
$E_{eq}$	Equilibrium potential
$\rho$	Density
$u$	Velocity
$p$	Pressure
$\tau$	The viscosity stress tensor
$\bar{D}$	Diffusivity
$c$	Concentration
$R'$	Generation or consumption rate

## 1. INTRODUCTION

Photo-driven reduction of CO<sub>2</sub> to produce fuel enables carbon sequestration and sustainable energy storage has drawn intensive research attentions[1]. Three pathways to reduce CO<sub>2</sub> with solar energy can be categorized, photocatalytic approach using single photocatalyst, photovoltaic powered electrolysis (PV-E),

direct photoelectrochemical (PEC) reduction[2]. Comparing with the other two approaches, PEC is regarded a promising configuration with more integrated architecture allowing direct light absorption at photoelectrode[3].

Generally, p-type semiconductors like Cu<sub>2</sub>O, GaP, SiC et.al are applied as photocathode in PEC to provide the photogenerated electrons for CO<sub>2</sub> reduction[4-6]. In order to drive the reduction half reaction at cathode, the conduction band of semiconductor should be more negative than the equilibrium potential of reduction. However, because the flat band at the surface of a certain kind of semiconductor is fixed, the overpotential for CO<sub>2</sub> reduction is unchangeable. Therefore, the kinetics of interfacial reduction reaction couldn't be accelerated through manipulating the potential of photocathode. The application of bias voltage between anode and photocathode can only enhance the charge carrier transfer performance within semiconductor and

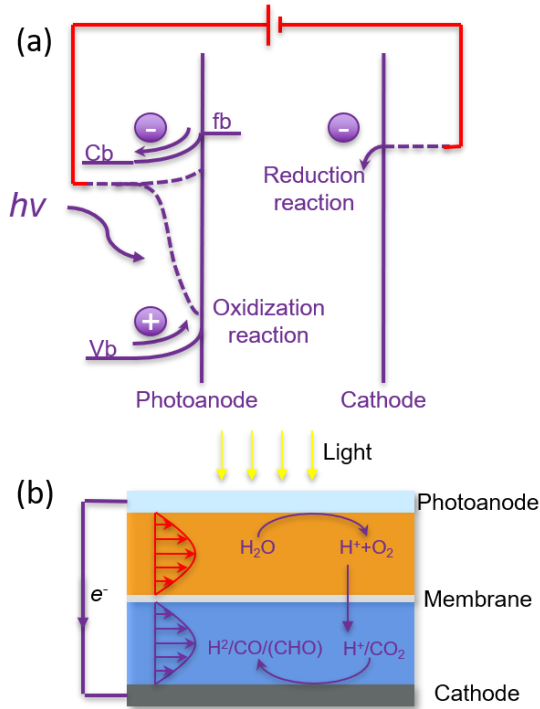


Fig 1 (a) Band structure of PEC with photoanode;  
(b) Schematic diagrams of PEC for CO<sub>2</sub> reduction

interfacial reaction at anode. This brings a great challenge on designing photocathode which should meet the multiple requirements of band gap position, the transfer performance of charge carrier in bulk semiconductor and interfacial reduction kinetics as well as hydrogen evolution suppression.

A PEC with n-type photoanode for CO<sub>2</sub> reduction is a promising way to take advantage of well-developed electrocatalyst for CO<sub>2</sub> reduction and enables direct light

absorption at the same time. N-type semiconductors are usually used as photoanodes in PEC which performs oxidation half reaction, such as oxygen evolution reaction (OER), by utilizing the oxidizing photoinduced holes[7]. While the concomitant photoelectrons transfer to the counter electrode. The reduction potential at cathode can be manipulated through adjusting the working potential of photoanode or applying bias, as shown in Fig. 1.

In this paper, a numerical model was built to study the performance of a PEC consists of a TiO<sub>2</sub> photoanode and metal cathode coated with Cu-In catalyst for CO<sub>2</sub> reduction[8]. The current-potential performance of both photoanode and cathode were studied to give an insight on interfacial kinetics. Through applying differential pH for cathode and anode, the PEC is able to work at self-contained condition with no bias voltage needed.

## 2. NUMERICAL MODEL

### 2.1 Governing equations

#### 2.1.1 Photoanode

The photocurrent generated at anode can be calculated by a modified Gartner-Butler expression which considering the recombination effect of electron-hole pairs at the surface of semiconductor[9,10].

$$j_{ph} = \Phi e I \left[ 1 - \frac{\exp(-\alpha \delta_{sc})}{1 + \alpha L} \right] \quad (1)$$

$$\delta_{sc} = \sqrt{\frac{2\epsilon\epsilon_0\Delta\phi_{sc}}{eN_d}} = \sqrt{\frac{2\epsilon\epsilon_0(V - V_{fb})}{eN_d}} \quad (2)$$

$$\Phi = \frac{R_i}{R_i + R_r} = \frac{A \exp(B \cdot \Delta\phi_{sc})}{1 + A \exp(B \Delta\phi_{sc})} \quad (3)$$

#### 2.1.2 Cathode

The electrochemical kinetics at cathode is governed by the Tafel equation as follows

$$j = -j_{0,c} \exp\left(-\frac{\beta F \eta}{RT}\right) \quad (4)$$

$$\eta = V - E_{eq} \quad (5)$$

#### 2.1.3 Hydrodynamics and Mass transfer

$$\nabla \cdot (\rho u) = -\nabla \cdot p + \nabla \cdot \tau \quad (6)$$

$$\nabla \cdot (\rho u) = 0 \quad (7)$$

$$\nabla \cdot (-\bar{D}_i \nabla c_i) + u \cdot \nabla c_i = R'_i \quad (8)$$

### 2.2 Boundary conditions and numerical solution

AM1.5G spectra was set as the incident light to excite TiO<sub>2</sub>, the light absorption properties of semiconductor

were obtained from Ref. [11]. The flow rate and saturated CO<sub>2</sub> concentration of electrolyte were set to solve the flow and mass transfer. The model was solved by Comsol Multiphysics.

### 3. RESULTS

#### 3.1 Model validation

The simulation *J-V* result of photoanode is compared with experimental data as shown in Fig. 2a. The good agreement indicates the validation of model on photoanode side.

As for the selected cathode, two major reduction products are hydrogen (10-20%) and carbon monoxide (80-90%). Since the hydrogen evolution kinetics on the surface of Cu-In is still unclear, it is unlikely to give concise numerical analyses on hydrogen evolution reaction. Furthermore, the hydrogen evolution reaction is unfavored and is suppressed efficiently especially at high current operation conditions. Therefore, a yield of hydrogen of 10% was assumed in this model. As shown in Fig. 2b, the simulated CO partial current density plot agrees well with the reported experimental data.

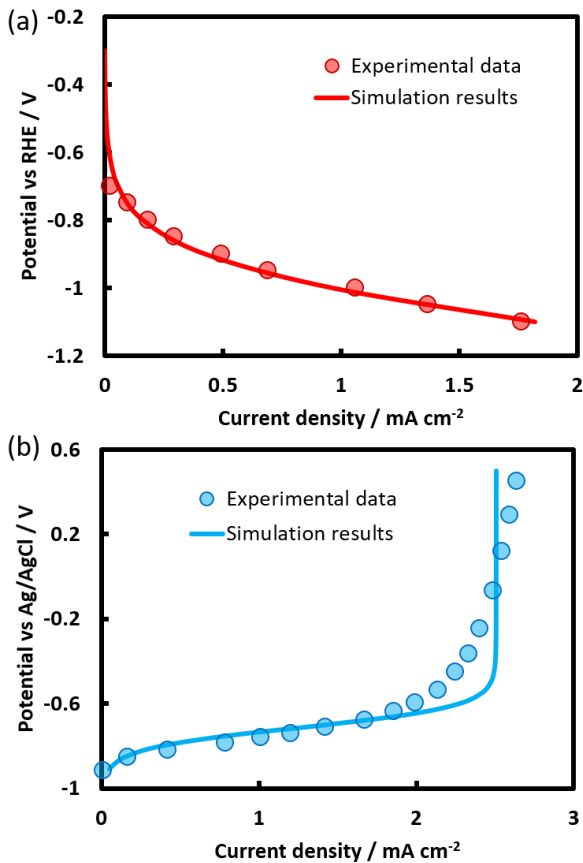


Fig 2 Comparisons of *J-V* performance between experimental data and simulation results: (a) CO reduction at cathode; (b) photoanode

#### 3.2 *J-V* characteristics

Fig. 3 shows the *J-V* curves of individual electrodes and whole cell at pH=7. For photoanode, in order to achieve the separation of electron-hole pairs, activation potential loss was necessarily needed to form a built-in electric field by bending the band gap. A limiting current density of 2.5 mA cm<sup>-2</sup> due to the charge carrier transfer performance within semiconductor will be reached with activation loss increasing. In contrast, no limiting current character was found within the current range at cathode because the current performance is still low and the CO<sub>2</sub>

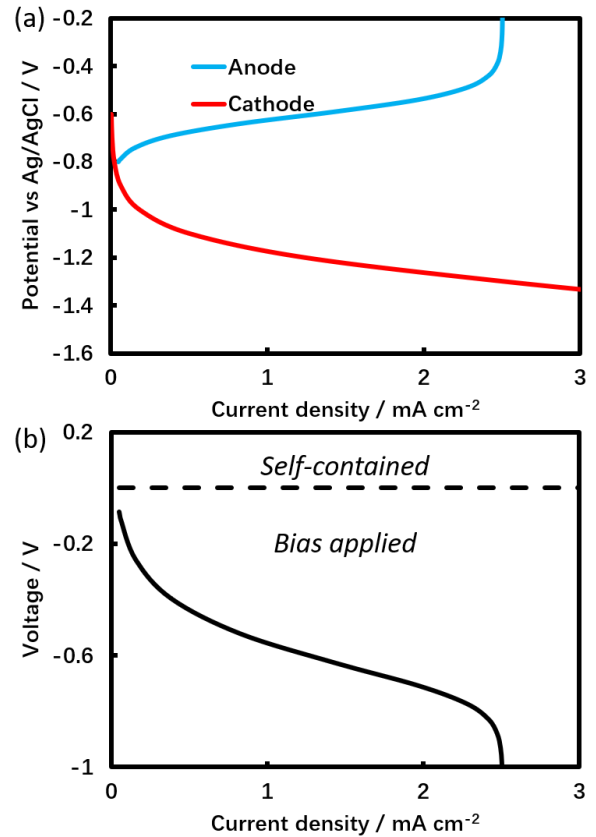


Fig 3 *J-V* performance of (a) anode and cathode, (b) whole cell

saturated solution supplies enough reactants for reduction.

It is found that when the flat potential of photoanode is more negative than the equilibrium potential at cathode, the photogenerated electrons can flow automatically from photoanode to the cathode driven by the potential difference between photoanode and cathode, under which circumstance, the PEC is self-contained with no bias necessary. Further increase in current performance can be obtained by applying bias

until  $2.5 \text{ mA cm}^{-2}$ . The photoanode performance is detected as the limiting factor of the device.

Although a self-contained working condition is favorable, the current performance is too low to meet the demand of carbon reduction and bias potential should be applied. This is because the potential difference between the anode and cathode is not sufficient to support high current performance. In order to increase the open circuit voltage, electrolytes of different pH can be implicated for anode and cathode. Alkaline solution is preferred to reduce the flat potential of photoanode, while the anodic equilibrium potential moving positive in acidic media. Theoretically, the maximum self-contained driving force of 1.1V can be obtained when alkaline (pH=14) and acid (pH=0) media are applied on cathodic and anodic stream respectively. Fig. 4 shows the cell performance of PEC at differential pH medias. The catalytic performance of cathode is assumed unchanged with pH. From the results, the PEC is found working self-contained till the limiting current of photoanode.

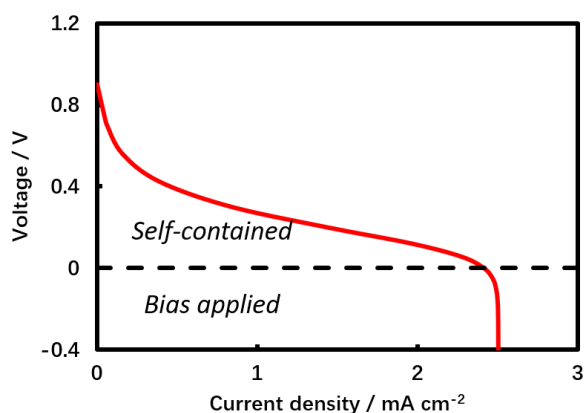


Fig 4 J-V performance of PEC at differential pH medias

#### 4. CONCLUSION

In this paper, a numerical model was present to study the performance of photoelectrochemical CO<sub>2</sub> reduction based on a n-type photoanode. Both of reduction kinetics and semiconductor charge transfer performance can be enhanced by applying bias voltage. Self-contained working condition can be achieved when the conduction band is more negative than the equilibrium of reduction reaction. By the means of adopting differential pH at photoanode and cathode, a maximum self-driven voltage of 1.1 V can be generated to perform CO<sub>2</sub> reduction.

#### ACKNOWLEDGEMENT

The research is supported by the UK Engineering and Physical Sciences Research Council (EPSRC) via grant number EP/R012164/2.

#### REFERENCE

- [1] Kumar B, Llorente M, Dang T, Sathrum A, Kubiak CP. Photochemical and photoelectrochemical reduction of CO<sub>2</sub>. *Annu Rev Phys Chem* 2012; 63:541–569.
- [2] Stolarczyk JK, Bhattacharyya S, Polavarapu L, Feldmann J. Challenges and Prospects in Solar Water Splitting and CO<sub>2</sub> Reduction with Inorganic and Hybrid Nanostructures. *ACS Catal* 2018; 8:3602–3635.
- [3] Qi J, Zhang W, Cao R. Solar-to-Hydrogen Energy Conversion Based on Water Splitting. *Adv Energy Mater* 2018; 8:1701620.
- [4] Schreier M, Luo J, Gao P, Moehl T, Mayer MT, Grätzel M. Covalent Immobilization of a Molecular Catalyst on Cu<sub>2</sub>O Photocathodes for CO<sub>2</sub> Reduction. *J Am Chem Soc* 2016; 136:1938–1946.
- [5] Lessio M, Carter EA. What Is the Role of Pyridinium in Pyridine-Catalyzed CO<sub>2</sub> Reduction on p-GaP Photocathodes? *J Am Chem Soc* 2015; 137:13248–13251.
- [6] Han C, Lei Y, Wang B, Wu C, Zhang X, Shen S, Sun L, Tian Q, Feng Q, Wang Y. The functionality of surface hydroxyls on selective CH<sub>4</sub> generation from photoreduction of CO<sub>2</sub> over SiC nanosheets. *Chem Comm* 2019; 55:1572–1575.
- [7] Wolcott A, Smith WA, Kuykendall TR, Zhao Y, Zhang JZ. Photoelectrochemical Water Splitting Using Dense and Aligned TiO<sub>2</sub> Nanorod Arrays. *Small* 2009; 5:104–111.
- [8] Rasul S, Anjum DH, Jedidi A, Minenkov Y, Cavallo L, Takanebe K. A Highly Selective Copper–Indium Bimetallic Electrocatalyst for the Electrochemical Reduction of Aqueous CO<sub>2</sub> to CO. *Angew Chem* 2015; 54:2146–2150.
- [9] Bedoya-Lora FE, Hankin A, Kelsall GH. En route to a unified model for photo-electrochemical reactor optimisation. I - Photocurrent and H<sub>2</sub> yield predictions. *J Mater Chem A* 2017; 5:22683–22696.
- [10] Hankin A, Bedoya-Lora FE, Ong CK, Alexander JC, Petter F, Kelsall GH. From millimetres to metres: the critical role of current density distributions in photo-electrochemical reactor design. *Energy Environ Sci* 2017; 10:346–360.
- [11] Wang G, Wang H, Ling Y, Tang Y, Fitzmorris RC, Wang C, Zhang JZ, Li Y. Hydrogen-Treated TiO<sub>2</sub> Nanowire Arrays for Photoelectrochemical Water Splitting. *Nano Lett* 2011; 11:3026–3033.